Photoaffinity ADP Analogs as Covalently Attached Reporter Groups of the Active Site of Myosin Subfragment 1†

Yin Luo,‡ Donald Wang,§ Christine R. Cremo,*,§ Edward Pate,‡ Roger Cooke,|| and Ralph G. Yount*,§

Departments of Pure and Applied Mathematics and of Biochemistry/Biophysics, Washington State University, Pullman, Washington 99164-4660, and Department of Biochemistry and Biophysics, University of California−San Francisco, San Francisco, California 94143

Received June 28, 1994; Revised Manuscript Received September 26, 1994⊗

ABSTRACT: The enzymatic properties of rabbit skeletal myosin subfragment 1 (S1) have been determined after photoaffinity labeling the active site with two ADP analogs. These analogs, 2-[(4-azido-2-nitrophenyl)-amino]ethyl diphosphate (NANDP) and the fluorescent analog 3′(2′)-*O*-(4-benzoylbenzoyl)-1,N^6-ethenoadenosine diphosphate ($Bz_2\epsilon$ADP), label the heavy chain residues Trp 130 and Ser-324, respectively. These residues in the crystal structure of chicken skeletal S1 are on either side of the entrance to the active site pocket (Rayment *et al.*, 1993b). Here S1 was photolabeled with NANDP or $Bz_2\epsilon$ADP after trapping with vanadate (Vi). Both of the photolabeled S1 preparations had normal MgATPase activities after removal of vanadate by actin treatment. These results show that the covalently tethered nucleotide analogs could move out of the active site and be replaced by MgATP. Experiments that monitored the fluorescence emission intensity, polarization, and quenching by acrylamide of S1 photolabeled with $Bz_2\epsilon$ADP show that the covalently linked analog was displaced out of the active site cleft by MgATP (or MgATP and actin) but not by ATP in the absence of Mg^{2+} ions. The effective concentration of the tethered ethenoadenosine diphosphate at the active site, determined by competition with MgATP, was calculated to be 10 mM. In the absence of Mg^{2+} ions, ATP was unable to compete with the bound analog. Binding constants of the S1 photolabeled with $Bz_2\epsilon$ADP to actin were 1.5×10^5 and 5.8×10^5 M^{-1} at 200 and 20 mM ionic strength, respectively, showing that actin binding affinities are similar to those obtained for S1•ADP. The binding of actin in the absence of MgATP did not produce any change in the emission intensity, polarization, or quenching by acrylamide of the tethered ethenoadenosine diphosphate, indicating that the conformation of the pocket around the adenine ring was unchanged. However, the binding of actin did destabilize Vi, which had been previously trapped in the form of photolabeled S1−Vi complexes. These results indicate that actin binding primarily affects the γ-phosphate binding site but not the adenine ring binding site.

Photoaffinity modification of S1[1] with photoreactive ATP or ADP and Pi analogs has been used to map the active site structure of myosin [reviewed in Yount *et al.* (1992)]. For example, trapped vanadate (Vi), an analog of phosphate, photooxidizes Ser-180 (Cremo *et al.*, 1989; Grammer *et al.*, 1988) and Ser-243 (Grammer & Yount, 1991) or rabbit skeletal S1 that, according to the crystal structure of chicken skeletal S1 (Rayment *et al.*, 1993b), are located at the bottom of the active site cleft. This suggests that the triphosphate portion of ATP should orient downward into the active site pocket with the γ-phosphate in close proximity of the serine residues. Photolabeling of Trp-130 by 2-azido-ATP (Grammer *et al.*, 1993) and NANDP (Okamoto & Yount, 1985) shows that this residue on the 23-kDa tryptic fragment of the heavy chain of rabbit skeletal S1 is close to the adenine ring of ATP. The photolabeling of Ser-324 by Bz_2ATP (Mahmood *et al.*, 1989) placed this residue near the ribose of bound ATP. Both of these latter residues reside at the entrance of the S1 active site pocket (Rayment *et al.*, 1993b).

NH_4^+-EDTA and K^+-EDTA ATPase activities of S1 are suppressed by the photoincorporation of NANDP (Okamoto & Yount, 1985), Bz_2ADP (Mahmood *et al.*, 1989), and other photoreactive ADP analogs. This loss of activity can be explained if NH_4^+- or K^+-ATP was unable to displace the covalently incorporated analogs from the active site. Following this reasoning, we expected that myosins photolabeled in permeabilized muscle fibers would be unable to contribute to force generation. Myosins modified in this way were expected to be in a state analogous to the actoS1•ADP state, which is regarded as the end of the power stroke. We predicted that heads of this type of myosin should not be dissociated (relaxed) from the actin filament upon the addition of MgATP in the absence of Ca^{2+}. Unexpectedly, skinned rabbit psoas fibers photolabeled to >40% with a

† Supported by grants from the Muscular Dystrophy Association (R.C. and R.Y.) and the NIH (DK 05195, R.Y.; AR 40917, C.R.C.; AR 39643, E.P.; HL 32145, R.C.). C.R.C. and E.P. are Established Investigators of the American Heart Association.

‡ Department of Pure and Applied Mathematics, Washington State University.

§ Department of Biochemistry/Biophysics, Washington State University.

|| Department of Biochemistry and Biophysics, UCSF.

⊗ Abstract published in *Advance ACS Abstracts,* January 15, 1995.

[1] Abbreviations: S1, myosin subfragment 1; NANDP, 2-[(4-azido-2-nitrophenyl)amino]ethyl diphosphate; ϵADP, 1,N^6-ethenoadenosine 5′-diphosphate; $Bz_2\epsilon$ADP, 3′(2′)-*O*-(4-benzoylbenzoyl)-1,N^6-ethenoadenosine 5′-diphosphate; Bz_2ADP, 3′(2′)-*O*-(4-benzoylbenzoyl)adenosine 5′-diphosphate; CBHϵADP, 3′(2′)-*O*-[[(phenylhydroxymethyl)phenyl]-carbonyl]ethenoadenosine 5′-diphosphate; CBHϵADP-S1 and NANDP-S1, S1 photolabeled with $Bz_2\epsilon$ADP or NANDP in the active site, respectively; Vi, orthovanadate; SDS−PAGE, sodium dodecyl sulfate−polyacrylamide gel electrophoresis; TCA, trichloroacetic acid; PAR, 4-(2-pyridylazo)resorcinol; BCA; bicinchoninic acid.

0006-2960/95/0434-1978$09.00/0

spin-labeled Bz_2ATP analog behaved virtually the same as the unmodified control (Wang *et al.*, 1994). The relaxed and active tension and stiffness as well as the maximum contraction velocity were not affected by the photolabeling. Similar studies of the mechanical properties of NANDP photolabeled fibers showed the same results (Y. Luo, *et al.*, unpublished results). These data suggested that, under the conditions of the fiber experiments, ATP could be hydrolyzed in a normal way by the photolabeled myosins.

To resolve the inconsistency between the S1 and fiber experiments, we reinvestigated the properties of $Bz_2\epsilon ADP$ (Cremo & Yount, 1987) and NANDP (Okamoto & Yount, 1985) photolabeled S1 under conditions which were close to those used for the fiber experiments, i.e., in the presence of actin and MgATP. The photolabeled S1 preparations had similar actin-activated MgATPase activity and actin binding affinity in the presence of MgATP as the unmodified control. These results show that MgATP in solution could enter the photolabeled active site and that the photolabeled residues were not essential for normal myosin function. In the absence of MgATP, binding to actin of the photolabeled S1 preparations was similar to that of the S1•ADP complex, consistent with the covalently labeled S1 being a stable analog of the S1•ADP state.

The fluorescence properties of $Bz_2\epsilon ADP$ labeled S1 (CBHϵADP-S1) were used to monitor the position of the ethenoadenine ring under varying conditions. When MgATP or MgATP plus actin was added to CBHϵADP-S1, the polarization and emission intensity decreased, and an increase in quenching by acrylamide was observed. These results show that the ethenoadenine ring of CBHϵADP-S1 was displaced out of the active site by MgATP to a more mobile and exposed position. Actin alone had no effect on the fluorescence properties of CBHϵADP-S1, indicating that actin binding has minimal effects on the adenine portion of the active site pocket. These studies show that it is possible to use the specificity of photoaffinity analogs to place reporter groups near the active site of an enzyme.

MATERIALS AND METHODS

The sources of commercial compounds were as follows: sodium adenosine triphosphate and chymotrypsins (Sigma); ultrapure urea, Schwarz/Mann Biotech; acrylamide, Bio-Rad; BCA Protein Assay Reagent, Pierce; ammonium molybdate, J.T. Baker; 4-(2-pyridylazo)resorcinol monosodium salt (PAR), Aldrich. The syntheses of [^{14}C]$Bz_2\epsilon ADP$ (Cremo & Yount, 1987), [^{3}H]NANTP, and [β-^{32}P]NANDP (Nakamaye *et al.*, 1985) were as described.

ATPase assays were performed as described previously (Wells *et al.*, 1979), except that the total phosphate in the assay mixture was analyzed at 2, 4, 6, and 8 min after the addition of S1. The ATPase rates were obtained from the linear least-square fit of the four points. The detailed assay conditions are specified in the legends. The concentrations of modified S1 were determined using the BCA assay with unmodified S1 as the standard. Liquid scintillation counting was performed on a Packard CA1900 scintillation counter with biodegradable scintillant (Amersham).

Protein Preparation. Rabbit skeletal myosin was prepared according to Wagner and Yount (1975) and stored in 50% glycerol at −20 °C. Chymotryptic S1 was prepared as described by Weeds and Taylor (1975) and was assumed to have a molecular weight of 115 000 and $\epsilon_{280}^{1\%} = 7.5$ cm^{-1} (Wagner & Weeds, 1977). F-actin was purified from rabbit skeletal muscle as described (Pardee & Spudich, 1982). To prepare ATP-free F-actin, F-actin was centrifuged in a Beckman TLA 100 ultracentrifuge at 350000*g* for 20 min at 4 °C, and the pellet was resuspended in ATP-free buffer containing 50 mM KCl, 10 mM Tris, 1 mM $MgCl_2$, 0.5 mM β-mercaptoethanol, and 0.005% NaN_3, pH 8.0, at 4 °C and then dialyzed vs 4 L of the same buffer for 24 h at 4 °C.

Enzyme Modification. [β-^{32}P]NANDP, [^{3}H]NANTP, or [^{14}C]$Bz_2\epsilon ADP$ was trapped at the active site of S1 after incubation for 20 min at room temperature with 1 mM Vi and 2 mM Co^{2+} as described (Cole & Yount, 1990). Co^{2+} was used instead of Mg^{2+} to avoid the undesired Vi-mediated photooxidation of serine residues at the active site (Grammer *et al.*, 1988). EDTA (20 mM) and ATP (20-fold excess over S1) were added, and untrapped analogs and Vi were removed by centrifugal gel filtration on a 5-mL Sephadex G-50 column (Penefsky, 1977) equilibrated in 100 mM KCl and 50 mM Tris, pH 8.0, at 4 °C (S1 buffer). The labeled S1 solutions were irradiated in a Petri dish on ice for 20 min with an Ace-Hanovia 450-W medium-pressure quartz mercury vapor lamp as described previously (Grammer *et al.*, 1988). The carbonyl group between the two benzene rings of $Bz_2\epsilon ADP$ is reduced to a tertiary alcohol upon photoincorporation onto S1 and is referred to as CBHϵADP-S1 (Cremo & Yount, 1987). The NANDP-labeled S1 is called NANDP-S1.

Removal of Noncovalently Bound Analog and Vi. After irradiation, the protein solution contained a mixture of unmodified S1, trapped but unmodified S1, and photolabeled S1. Actin was used to dissociate the trapped analogs and Vi from the active site. F-actin (1 mL, 100 μM) was pelleted by centrifugation in a Beckman TLA 100 ultracentrifuge at 350000*g* and 4 °C for 10 min. The supernatant was discarded, and 1 mL of an irradiated S1 solution at low ionic strength (10−50 mM KCl) was added and used to resuspended the F-actin pellet. Following the addition of 2 mM $MgCl_2$ and 2 mM NaATP (pH 7.0), the solution was incubated at room temperature for 20 min to release trapped Vi and the unincorporated analogs. ATP was added again (final concentration 4 mM), and the ionic strength was increased to 200 mM by the addition of 3 M KCl, while the temperature was lowered to 4 °C to provide more favorable conditions for the dissociation of S1 and photolabeled S1 from actin. The solution was immediately centrifuged at 350000*g* for 20 min at 4 °C as above. The supernatant was applied to a 5-mL Sephadex G-50 centrifugal column following the addition of 0.5 M EDTA to 20 mM to remove Mg^{2+}, ATP, Vi, and the released unincorporated nucleotide analog. The resulting solution contained unmodified S1 and photolabeled S1 and is called the purified CBHϵADP-S1 or purified NANDP-S1 as appropriate.

The molar ratio of radiolabeled analog to S1 (equivalent to the initial percent of trapping) in the irradiated solution prior to actin purification was determined by direct scintillation counting. The percent covalent incorporation at this stage was determined as follows: an aliquot of sample was precipitated with an equal volume of 10% trichloroacetic acid. The pellet was washed twice with 5% trichloroacetic acid and dissolved in a solution of 4% SDS and 1 M Tris, pH 10, before the scintillation counting.

Table 1: Characterization of the Species Present in Irradiated Solutions before and after Actin−MgATP Purification

	before purification			after purification		
ADP analog	L-S1/S1$_t$[a]	L*S1/S1$_t$[b]	Vi/S1$_t$[c]	L-S1/S1$_t$[a]	L*S1/S1$_t$[b]	Vi/S1$_t$[d]
L = [^{3}H]NANDP	0.55	0.27	0.79	0.48	0.04	0.0
L = [^{14}C]Bz$_2\epsilon$ADP	0.62	0.11	0.68	0.60	0.03	0.0

[a] L-S1 represents S1 covalently labeled with ADP analog. S1$_t$ is the total S1 in solution. The values were calculated from radioactivity measurements after TCA precipitation (see Methods). [b] L*S1 represents S1 with trapped ADP analog but not covalently incorporated. The values were calculated from the difference in radioactivity of the irradiated sample before and after TCA precipitation. [c] Mole of Vi per mole of S1 was determined by the PAR assay as described in Materials and Methods. The Vi/S1$_t$ values reflect the initial amounts of Vi trapped and are equal to the initial amounts of ADP analog trapped. [d] Amount of Vi after actin purification step.

The free and total Vi concentrations were determined by the PAR colorimetric method (Goodno, 1979). Since the Co^{2+}−PAR complex has interfering absorbance, a Co^{2+} standard was measured in parallel with a Vi standard, and its absorbance was subtracted from measurements for the unpurified labeled S1 sample assuming the Co^{2+} concentration was the same as the total nucleotide concentration.

Binding Constants of Photolabeled S1 to Actin. The binding of photolabeled S1 (1 μM) to actin (10−100 μM) was measured using a sedimentation method (Biosca *et al.*, 1986). The protein solutions were centrifuged for 20 min on a Beckman TLA 100 ultracentrifuge at 350000*g* and 22 °C. The supernatants were then assayed for radioactivity to obtain the concentration of unbound labeled S1. The total concentration of the photolabeled S1 was calculated from the percentage of labeling. In control samples in which actin was not added, the concentration of the labeled S1 in the supernatant after centrifugation was the same as the initial concentration before centrifugation. Therefore, no correction for binding in the absence of actin was applied to the data. The simple binding equilibrium (eq 1)

$$\text{L-S1} + \text{actin} \rightleftarrows \text{actin·L-S1} \qquad K_a = \frac{[\text{actin·L-S1}]}{[\text{L-S1}][\text{actin}]} \quad (1)$$

where L denotes the incorporated diphosphate photoaffinity labels leads to eq 2, which can be used for calculating the binding constant, K_a.

$$\frac{[\text{L-S1}]_{\text{total}}}{[\text{L-S1}]_{\text{bound}}} = \frac{1}{K_a[\text{actin}]_{\text{free}}} + 1 \quad (2)$$

The concentration of bound labeled S1 in eq 2 was calculated from the difference between the total and the unbound labeled S1. Initially, $[\text{actin}]_{\text{free}}$ was corrected for the binding of unmodified S1, assuming 0% and 100% binding in the presence and absence of ATP, respectively. This correction was found to be negligible here because actin was in a large excess over total S1.

Fluorescence Measurements. Fluorescence measurements were made at 20 °C with an SLM 4800 fluorometer (SLM Instruments, Urbana, IL) interfaced with a computer. See figure legends for other conditions.

RESULTS

Purification and Characterization of NANDP-S1 and CBHϵADP-S1. To characterize the NANDP-S1 and CBHϵADP-S1 formed by irradiation of the Co^{2+}−analog−Vi complexes, it was essential to first remove the residual Vi and trapped unactivated nucleotide. It is known that actin destabilizes the Vi trapped nucleotide complexes (Goodno & Taylor, 1982), and our preliminary experiments showed that NANDP-S1 and CBHϵADP-S1 bound to F-actin in an ATP dependent manner. Accordingly, irradiated samples were mixed with F-actin at low ionic strength to release trapped Vi and ADP analog prior to adding excess ATP to dissociate S1 and photolabeled S1 from the F-actin. The samples were then centrifuged, and the supernatant, containing 80−90% of the initial S1, was purified by gel filtration. The amount of actin in the supernatant was less than 1% of the total protein as determined by densitometric scanning of SDS gels (data not shown).

Table 2: ATPase Activities of Vi-Trapped Labeled S1 Preparations at 25 °C

assay	[^{3}H]NANDP-S1[a]	[^{14}C]CBHϵADP-S1[a]
Vi/S1[b]	0.56	0.53
MgATPase[c] (% of control)[d]	62	44
MgATPase+ actin[e] (% of control)	106	105

[a] A total of 17 μM [^{3}H]NANDP-S1 (53% photolabeled) or [^{14}C]CBHϵADP-S1 (52% photolabeled) was treated with 1 mM Vi for 30 min at 25 °C in 2 mM $MgCl_2$ and 10 mM Hepes, pH 7.0. Excess Vi was removed as described in Materials and Methods prior to all assays. [b] Mole of Vi per mole of S1 was determined by the PAR assay as described in Materials and Methods. [c] Assays were performed as described in Materials and Methods in 2 mM $MgCl_2$, 1 mM ATP, and 10 mM Hepes, pH 7.0. [d] Unmodified S1. [e] Assays were performed as described in Materials and Methods in 5 mM $MgCl_2$, 5 mM ATP, and 10 mM Hepes, pH 7.0, with 10 and 23 μM actin for [^{3}H]NANDP-S1 and [^{14}C]CBHϵADP-S1, respectively.

To ensure that the purification procedure released Vi and unincorporated label, we measured the amount of trapped Vi, trapped analog, and covalent labeling before and after the actin purification step. Table 1 shows two examples of such measurements for NANDP-S1 and CBHϵADP-S1. The amount of trapped Vi before actin purification was comparable with the total amount of analog in the sample. But after the actin−MgATP treatment, Vi was completely eliminated, and the level of noncovalently bound analog decreased to less than 5% of the total S1. Therefore, this partial purification procedure typically gives preparations which contain between 40% and 60% photolabeled S1 with the remaining S1 unmodified.

It was of interest to test whether Vi can be trapped at the active site in the presence of a covalently attached nucleotide (Table 2). Labeled S1 preparations (similar to those in Table 1, after purification) were treated with 1 mM Vi and 2 mM $MgCl_2$ for 30 min at 25 °C. Table 2 shows that the mole fraction of Vi incorporated into each labeled S1 preparation agreed well with the amount of covalently attached analog. This indicates that both ADP analogs tethered to S1 can function like free ADP to reform stable Vi complexes. The

Table 3: ATPase Activities [(μmol of Pi) mg^{-1} min^{-1}] of Photolabeled S1 Preparations at 25 °C

ATPase conditions	[^{3}H]NANDP-S1			[^{14}C]CBHϵADP-S1		
	control[a]	labeled[b]	% of control	control[a]	labeled[b]	% of control
NH_4^+-EDTA[c]	14.10	8.46	60	13.8	5.38	39
NH_4^+-EDTA + actin[d]	11.30	6.44	57	11.9	5.36	45
K^+-EDTA[e]	2.93	1.20	41	2.60	0.96	37
K^+-EDTA + actin[f]	0.64	0.36	57	1.34	0.54	40
Mg^{2+} [g]	0.033	0.039	118	0.025	0.028	113
Mg^{2+} + actin[h]	2.95	3.48	118	4.16	4.58	110

[a] Unmodified S1. The results were the same with or without UV irradiation as has been previously shown (Nakamaye *et al.*, 1985; Cremo & Yount, 1987). [b] Samples were partially purified by treatment with MgATP and actin as described in Materials and Methods. NANDP-S1 is 48% labeled, and CBHϵADP is 59% labeled. [c] 0.56 M NH_4Cl, 0.23 M KCl, 38 mM EDTA, 62.5 mM Tris, and 6 mM ATP, pH 8.0. [d] Conditions were the same as in footnote *c*, except for the addition of 10 μM actin to [^{3}H]NANDP-S1 and 6 μM actin to [^{14}C]CBHϵADP-S1. [e] 0.6 M KCl, 50 mM, 5 mM EDTA, 50 mM Tris, and 5 mM ATP, pH 7.5. [f] The buffer conditions were the same as in footnote e, and the actin concentrations were the same as in footnote d. [g] 10 mM HEPES, 2 mM $MgCl_2$, and 1 mM ATP, pH 7.0. Phosphate was measured by the malachite green assay as described (Lanzetta *et al.*, 1979). [h] 10 mM HEPES, 5 mM $MgCl_2$, and 5 mM ATP, pH 7.0, 10 and 48 μM actin were used with [^{3}H]NANDP-S1 and [^{14}C]CBHϵADP-S1, respectively.

MgATPase activities (Table 2) of the Vi-treated labeled S1 preparations were lower than control values (unmodified S1). These activities agree reasonably well with the fraction of unmodified S1 present in each labeled S1 preparation. This indicates that the enzymatically inactive Vi complexes remained essentially stable during the assay. Addition of actin, however, stimulated the MgATPase activities of the control and Vi-treated labeled S1 preparations to the same level. These results show that the addition of actin plus MgATP but not MgATP alone will rapidly destabilize the photolabeled S1-Vi complexes.

Binding Constants of Purified Labeled S1 to Actin. As the purified labeled preparations appeared to be good analogs of S1-ADP, it was of interest to measure their actin binding affinities. Figure 1 shows a double-reciprocal plot of the binding of NANDP-S1 and CBHϵADP-S1 over a limited range of actin concentrations. The use of higher actin concentrations was limited by the specific radioactivities of the radiolabeled nucleotides. The apparent affinity constants, estimated from the reciprocal of the slopes were 1.5×10^5 M^{-1} at 200 mM ionic strength for NANDP-S1 and 5.8×10^5 M^{-1} at 20 mM ionic strength for both NANDP-S1 and CBHϵADP-S1. The *y*-intercepts of these plots (which were above 1.0) were not used to calculate stoichiometry of binding because of the sensitivity of the intercept to small amounts of free nucleotide present in the labeled S1 samples. The affinity of CBHϵADP-S1 could not be measured accurately at 200 mM ionic strength because of the low specific radioactivity of CBHϵADP. The binding constant was estimated to be 1.5×10^5 M^{-1} (data not shown). Similarly, in the presence of ATP, the affinity constants of both NANDP-S1 and CBHϵADP-S1 were too low to be accurately measured, but ranged from 1×10^3 to 6×10^3 M^{-1} based on the averaged percent binding of labeled S1 to actin at both ionic strengths (data not shown). These values are within the range measured for the binding of actin to native S1-ATP [1×10^3 M^{-1} (Geeves *et al.*, 1984); 5×10^2 M^{-1} (Millar & Geeves, 1988); 1.5×10^4 M^{-1} (Chalovich & Eisenberg, 1982)]. The normal ATP-dependent actin binding of the photolabeled preparations was consistent with the fact that photolabeled fibers had normal mechanical properties (Wang *et al.*, 1994; D. Wang *et al.*, in preparation). This suggested that the photolabeling method described here may be an excellent method to specifically attach extrinsic reporter groups to S1 without drastic modification of the protein. This led to the following investigation of the enzymatic properties of these photolabeled preparations.

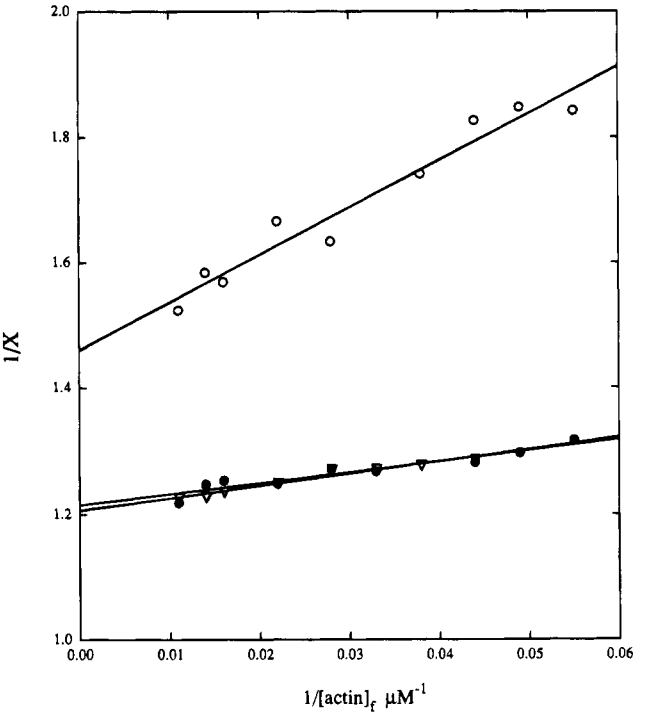

FIGURE 1: Actin binding to photolabeled S1 preparations. Double-reciprocal plot of the binding of the [^{3}H]NANDP-S1 (51% labeling) and [^{14}C]CBHϵADP-S1 (60% labeling) to actin in the absence of ATP. These samples are similar to those described in Table 1 (after actin purification). $X = [L\text{-}S1]_{bound}/[L\text{-}S1]_{total}$ (Methods), where L stands for NANDP or CBHϵADP. At 200 mM ionic strength (0.17 M KCl, 8 mM $MgCl_2$, 1 mM EGTA, 40 mM MOPS, pH 7.0), the binding of [^{3}H]NANDP-S1 (○) fit to a binding constant of 1.5×10^5 M^{-1}. At 20 mM ionic strength (10 mM KCl, 3 mM $MgCl_2$, 1 mM EGTA, 40 mM MOPS, pH 7.0), both [^{3}H]NANDP-S1 (●) and [^{14}C]CBHϵADP-S1 (▽) fit to a binding constant of 5.8×10^5 M^{-1}. Total [S1] = 1.0 μM, T = 20 °C.

Enzymatic Activities of Purified NANDP-S1 and CBHϵADP-S1. The ATPase activities of the purified labeled preparations are given in Table 3. Because the activity of the labeled S1 relative to a control sample varied with the labeling percentage, for clarity, only one set of data for each analog is shown. Replicate data sets showed similar behavior. Both photolabeled preparations had reduced NH_4^+-EDTA and K^+-EDTA ATPase activities in proportion to the percentage of labeling. For example, CBHϵADP-S1 was 59% labeled and

had NH_4^+-EDTA and K^+-EDTA ATPase activities of 39% and 37% of the controls, respectively (Table 3). The activity in the labeled S1 preparation could be attributed to the presence of unmodified S1. Therefore, the labeled S1 appeared to have negligible NH_4^+-EDTA and K^+-EDTA ATPase activity. This result was not unexpected, as similar effects of photolabeling upon these ATPase activities have been demonstrated previously (Cremo & Yount, 1987; Mahmood *et al.*, 1989; Nakamaye *et al.*, 1985).

The photolabeled preparations were not irreversibly inactivated, because in the presence of Mg^{2+}, the ATPase activities were the same as or slightly higher for both NANDP-S1 and CBHϵADP-S1 than that of the controls. (The 10−20% higher activities of the labeled preparations compared to the control may be due to the removal of some nonfunctional S1 by the actin−MgATP purification step prior to the assay.) For all three assay conditions, the addition of actin caused the same changes in the control as in the labeled S1 preparation (Table 3). This suggests that the activities of the NANDP-S1 and the CBHϵADP-S1 present in the labeled S1 preparations were the same as the control S1. In addition, the activities of the labeled preparations in terms of percentage of the controls were not effected by actin. The key finding from the data in Table 3 is that both photolabeled preparations can hydrolyze ATP in the presence of Mg^{2+} at the normal rate even though the active site has been covalently photolabeled with the ADP analogs.

These data (Table 3 and Figure 1) shows that the analogs can be released from the active site in such a manner as to allow MgATP to compete for the site. From the structure of the active site (Rayment *et al.*, 1993a) and the locations of the amino acids photolabeled, we predicted that the displaced probes would become more mobile and exposed to the solvent upon the addition of MgATP. To test hypothesis, we examined the effect of MgATP upon the fluorescence properties of CBHϵADP-S1. This approach also allowed us to ask the question as to whether actin alone in the absence of MgATP could have a similar effect.

Fluorescence Polarization of CBHϵADP-S1. We used fluorescence polarization to measure the effect of ATP and actin upon the mobility of the ϵATP reporter group of CBHϵADP-S1 (Figure 2). It is known that the polarization of Bz_2ϵADP increases upon binding reversibly to or trapping at the active site of S1 (Cremo & Yount, 1987), which indicates a decrease in the mobility of the probe. Figure 2 demonstrates this decrease in mobility of the Bz_2ϵADP upon trapping with Vi (compare a and b).

CBHϵADP-S1 (c) had a high polarization value similar to the trapped nucleotide. From the data in Table 3, we predicted a decrease in polarization upon the addition of MgATP but not K^+ ATP to the CBHϵADP-S1. As expected, the addition of MgATP to the CBHϵADP-S1 decreased the polarization (f), whereas K^+ ATP did not have an effect (e). The polarization of the CBHϵADP-S1 treated with MgATP (f) is higher than the CBHϵADP-S1 in the presence of 6 M urea (g), suggesting that the mobility of the covalently attached probe is limited by the rotational correlation time of S1, as expected.

The polarization of CBHϵADP-S1 (c) did not change upon the addition of 5 μM actin (h). The binding constant of CBHϵADP-S1 to actin at the ionic strength used in this experiment can be estimated from the data in Figure 1 as 3.7×10^5 M^{-1}. Therefore at 2 μM S1 and 5 μM actin, we estimate that 62% of the S1 in (h) is bound to actin. We would have expected the polarization of (h) to decrease to about 0.20 if the motion of the ϵADP reporter group in the CBHϵADP-S1−actin complex was increased as it was in the presence of MgATP (f). In the presence of actin, MgATP caused the same decrease in polarization (j) as was seen in the absence of actin (f). Neither NH_4^+ ATP nor K^+ ATP significantly changed the polarization either in the presence of actin (i) or the absence of actin (e). Thus, the specific effect of MgATP to increase the mobility of the nucleotide in CBHϵADP-S1 was not mimicked by or altered in the presence of actin.

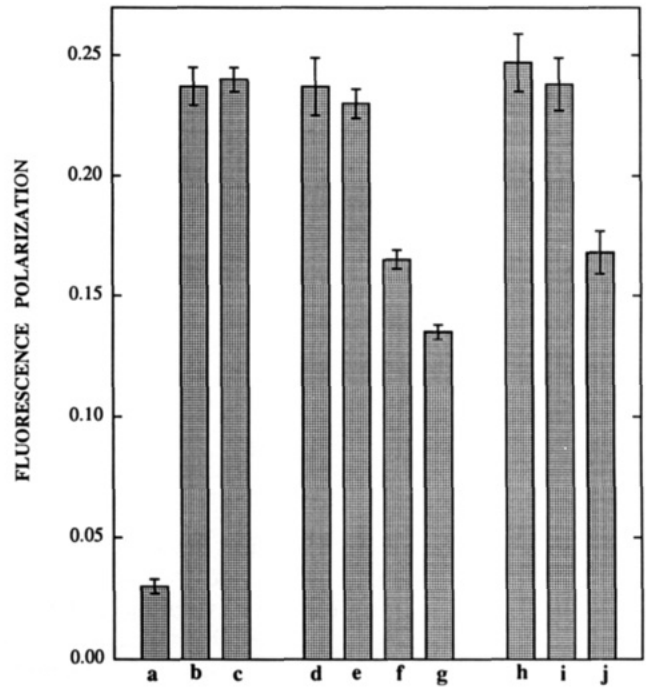

FIGURE 2: Emission polarization of ϵADP derivatives. (a) free Bz_2ϵADP in buffer; (b) Co^{2+}·Bz_2ϵADP·Vi·S1 complex; (c) CBHϵADP-S1; (d) CBHϵADP-S1 + 0.8 mM EDTA; (e) d + 2 mM K^+ ATP; (f) e + 2 mM $MgCl_2$; (g) f + urea to 6 M; (h) CBHϵADP-S1 + 5 μM F-actin; (i) h + 0.6 M NH_4Cl, 0.3 M EDTA, and 2 mM ATP; (j) CBHϵADP-S1 + 5 μM actin + 2 mM $MgCl_2$ + 2 mM ATP. The error bars represent the standard deviation from the mean of three to six experiments. Within a single experiment, 9−13 replicate measurements of emission intensity were acquired by computer at each polarizer setting until the accumulated standard deviation was lower than 0.5%. In all measurements, total [S1] = 2.0 μM, with 75% S1 trapped with Bz_2ϵADP in b or 59−61% S1 photolabeled as CBHϵADP-S1 in c−j. 5 μM actin was chosen for h−j in order to maintain both a reasonable excess of actin over CBHϵADP-S1 and a negligible increase in polarization due to an increase in viscosity. Addition of 5 μM F-actin to free Bz_2ϵADP increased the polarization by 0.01. Buffer contained 0.1 M KCl and 50 mM Tris − Cl, pH 8.0. T = 20 °C. The excitation wavelength was 330 nm with an 8-nm bandwidth; fluorescence emission was detected through 408-nm cutoff filters in a T-format.

As predicted from the data in Table 2, the addition of MgATP to the CBHϵADP-S1·Vi complex did not change the polarization significantly (data not shown). However, further addition of actin decreased the polarization to 0.17. This shows that actin binding affected the stability of the Vi in the CBHϵADP-S1·Vi complex as has been previously shown for the ADP·Vi·S1 (Goodno & Taylor, 1982). This destabilization of the Vi then allows MgATP to effectively compete for the active site which displaces the CBHϵADP to a more mobile position.

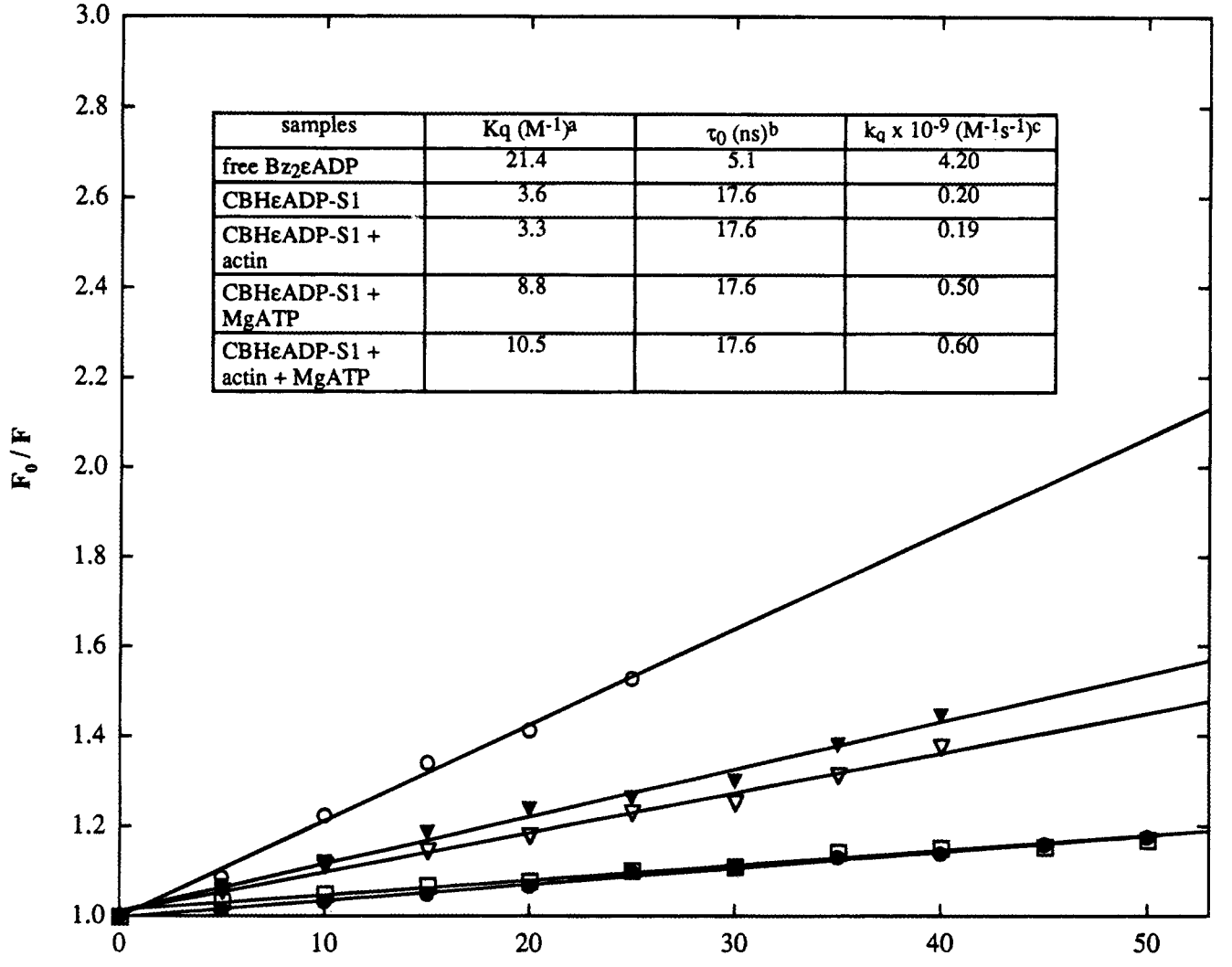

samples	Kq (M^{-1})[a]	τ_0 (ns)[b]	$k_q \times 10^{-9}$ ($M^{-1}s^{-1}$)[c]
free $Bz_2\epsilon$ADP	21.4	5.1	4.20
CBHϵADP-S1	3.6	17.6	0.20
CBHϵADP-S1 + actin	3.3	17.6	0.19
CBHϵADP-S1 + MgATP	8.8	17.6	0.50
CBHϵADP-S1 + actin + MgATP	10.5	17.6	0.60

FIGURE 3: Stern–Volmer plots of acrylamide quenching of the fluorescence of ϵADP derivatives. $Bz_2\epsilon$ADP (20 μM) in buffer (○), CBHϵADP-S1 (●), CBHϵADP-S1 + 5 μM actin (□), CBHϵADP-S1 + 2 mM MgATP (▽), and CBHϵADP-S1 + 5 μM actin + 2 mM MgATP (▼). The excitation and emission wavelengths were 330 and 402 nm, respectively, both with an 8-nm bandwidth. No polarizers were used. Total [S1] = 2.0 μM with 61% photolabeled. An ATP regenerating system, 1 mg/mL creatine kinase and 20 mM creatine phosphate, was used in all the measurements except CBHϵADP-S1 + 5 μM actin. The buffer conditions and temperature were the same as in Figure 2. Inset: Tabulation of Stern–Volmer quenching constants and calculation of bimolecular quenching constants (k_q). Footnote *a*: K_q values are calculated from the data in this figure. Footnote *b*: τ_0 values are average lifetimes taken from Cremo and Yount (1987) for Vi-trapped CBHϵADP on S1. Note that the average τ_0 for free CBHϵADP was 23.5 ns. Footnote *c*: See Results for equation to calculate k_q.

Acrylamide Quenching of CBHεADP-S1 Fluorescence. We examined the acrylamide quenching of the fluorescence to test whether the increase in mobility (Figure 2) of the CBHϵADP in CBHϵADP-S1 caused by MgATP was coupled to a change in the accessibility of the fluorophore to the solvent (Figure 3). The conditions of the experiment parallel those in Figure 2. The data were plotted according to Stern–Volmer (eq 3; (Lehrer & Leavis, 1978; Stern & Volmer, 1919)):

$$F_0/F = 1 + K_q[Q] = 1 + k_q\tau_0[Q] \qquad (3)$$

where F_0 and F are fluorescence intensities in the absence and presence of quencher, respectively, K_q is the Stern–Volmer constant, k_q is the bimolecular quenching constant, τ_0 is the lifetime, and [Q] is the concentration of acrylamide. The linear nature of these data suggests that the quenching mechanism is primarily collisional. The Stern–Volmer quenching constants (K_q) obtained from these plots and the estimated lifetimes (τ_0) (Cremo & Yount, 1987) were used to calculate the bimolecular quenching constants (k_q; Figure 3, inset). CBHϵADP-S1 had a k_q of 0.2 M^{-1} s^{-1}, which is about a factor of 20 lower than that observed for the free fluorophore. The addition of actin to CBHϵADP-S1 did not significantly effect the k_q. However, the addition of MgATP alone or the combination of MgATP and actin to CBHϵADP-S1 increased the k_q significantly by about a factor of 2–3, indicating an increased accessibility of the nucleotide to the solvent and the quencher, assuming that the quenching efficiency remained the same. These latter two values are the lower limits of our estimate of k_q as we have used the lifetime of Vi trapped CBHϵADP in the calculation. These data are consistent with the idea that MgATP displaces the covalently bound fluorophore from the active site to a position that is more accessible to the quencher in the solvent.

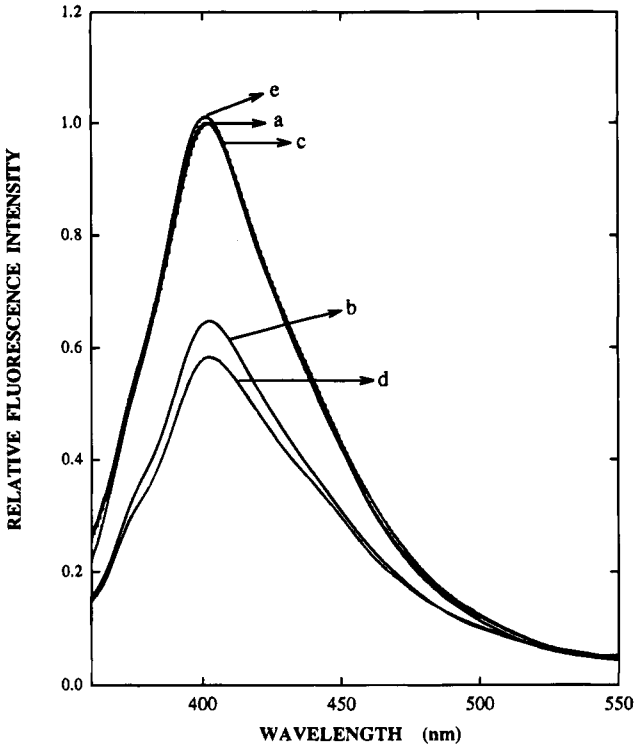

FIGURE 4: Fluorescence emission spectra. (a) CBHϵADP-S1; (b) CBHϵADP-S1 + 2 mM MgATP; (c) CBHϵADP-S1 + 5 μM actin; (d) c + 2 mM MgATP; (e) d after 20 min. Total [S1] = 11.7 μM, with 61% photolabeled as CBHϵADP-S1. No polarizers were used. The use of polarizers at the magic angle did not change the data. Other conditions were the same as in Figure 2, except that the emission was detected through a monochromter and a 4-nm bandwidth was used for both excitation and emission monochrometers. All spectra were normalized to the spectrum of a.

Fluorescence Intensity of CBHϵADP-S1. We examined the fluorescence emission spectra of CBHϵADP-S1 as an additional tool to probe the microenvironment of the fluorophore. The addition of MgATP decreased the emission intensity maximum of the CBHϵADP-S1 at 402 nm by about 35% (Figure 4; compare a and b). Addition of F-actin alone (c) did not change the intensity of CBHϵADP-S1. The combination of F-actin and MgATP (d) caused the emission to decrease initially by about 42% of CBHϵADP-S1, but after hydrolysis of all the ATP (as confirmed by thin-layer chromatography analysis), the fluorescence returned to the initial level (e). The addition of NH_4^+ ATP or K^+ ATP to CBHϵADP-S1 did not have a measurable effect on the emission intensity (data not shown). The pattern of changes in emission intensities correlated with both the polarization (Figure 2) and the acrylamide quenching data (Figure 3), suggesting that emission intensity was reporting the steady-state turnover of MgATP in the active site after it displaces the covalently bound probe. These studies also show that CBHϵADP tethered to S1 reenters the active site after all the ATP is hydrolyzed.

The decrease in emission intensity caused by MgATP was used to measure the effective concentration of the CBHϵADP at the active site of CBHϵADP-S1 (Figure 5). We denote the intensity decrease (at 402 nm) relative to the intensity in the absence of MgATP as ΔF and the ΔF at 2 mM MgATP as ΔF_{max}. The relative intensity change, *i.e.*, $\Delta F/\Delta F_{max}$, is plotted as a function of [MgATP]. $\Delta F/\Delta F_{max}$ is assumed to be proportional to the fraction of the active sites of CBHϵADP-S1 that are occupied by MgATP. The open and

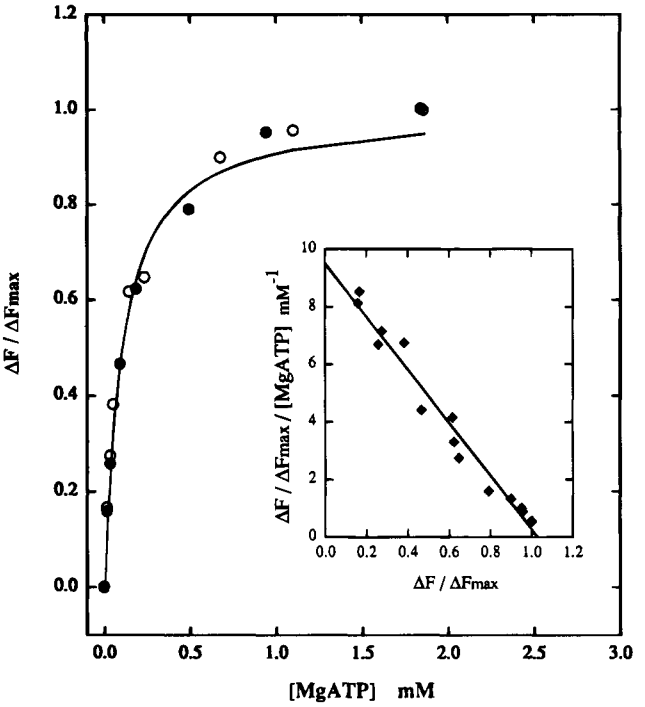

FIGURE 5: Measurement of the effective concentration of CBHeADP at the active site of CBHϵADP-S1. Relative fluorescence emission intensity of CBHϵADP-S1 at 402 nm is plotted as a function of [MgATP]. See Results for definitions of variables. The open and filled circles are two independent sets of data. The solid line is a fit of all data points to the equation $\Delta F/\Delta F_{max} = K[MgATP]/(1 + K[MgATP])$ (see Discussion), with a fitted K of 9.7×10^3 M^{-1}. Inset: All data points in Figure 3 are plotted according to the Scatchard equation (Discussion), $\Delta F/\Delta F_{max}/[MgATP] = K(1 - \Delta F/\Delta F_{max})$. A linear fit provides a K value of 9.2×10^3 M^{-1}. All spectra were corrected for dilution. Total [S1] = 8.6 μM with 51% photolabeled as CBHϵADP-S1. [creatine kinase] = 1 mg/mL; [creatine phosphate] = 10 mM. Excitation wavelength was 330 nm with an 8-nm bandwidth used with both excitation and emission monochrometers. No polarizers were used. The temperature and buffer were the same as in Figure 2.

filled circles represent two sets of independent data. A Scatchard plot, *i.e.*, $\Delta F/\Delta F_{max}/[MgATP]$ versus $\Delta F/\Delta F_{max}$, using all points from both data sets is shown in the inset of Figure 5. The slope of the fitted line, *i.e.*, the K in the Scatchard equation $\Delta F/\Delta F_{max}/[MgATP] = K(1 - \Delta F/\Delta F_{max})$, is 9.2×10^3 M^{-1}. The solid curve in Figure 5 is a least-square fit to the same equation but in the form $\Delta F/\Delta F_{max} = K[MgATP]/(1 + K[MgATP])$, with a fitted K of 9.7×10^3 M^{-1}. The interpretation of the above Scatchard equation will be given in the Discussion.

DISCUSSION

Our first goal was to obtain purified preparations of NANDP-S1 and CBHϵADP-S1. In initial experiments, we noticed that the binding of NANDP-S1 and CBHϵADP-S1 to actin was ATP dependent. This finding led to the use of actin and MgATP to purify the photolabeled proteins in high yield (Table 1). This purification scheme removed unincorporated ADP analogs and Vi while preserving the initial extent of photolabeling. Typically, this gave preparations which contained about 50% labeled and 50% native S1.

With the purified labeled preparations, in which only the stable photoadduct was radioactive, it was straightforward to measure directly the binding of the photolabeled proteins to actin (Figure 1). In the absence of ATP, the apparent

association constant of NANDP-S1 to F-actin (1.5×10^5 M^{-1}) was very close to that of S1•ADP (1.3×10^5 M^{-1}) (Greene & Eisenberg, 1980) at 200 mM ionic strength and 22 °C. At 20 mM ionic strength, the binding constant for the labeled S1 (5.8×10^5 M^{-1}) is somewhat tighter but comparable to values obtained at 100 mM KCl, pH 7−8 and 20 °C (~5×10^5 M^{-1}) (Geeves, 1989; Siemankowski & White, 1984; Trybus & Taylor, 1980). In the presence of MgATP, both NANDP-S1 and CBHϵADP-S1 had similar low affinities to F-actin as does native S1 or S1•ADP, with K_a values on the order of 10^3 M^{-1} (data not shown). Therefore, the binding of covalently labeled preparations to actin was found to be similar to that of the reversibly bound S1•ADP complex.

The relatively normal actin binding constants (Figure 1) show that the covalently attached ADP analog is bound correctly in the active site, producing a similar perturbation on the actin affinity as does ADP. The normal MgATPase activities (Table 3) of the photolabeled S1 preparations suggest that the Ser-324 (for Bz_2ϵADP) and Trp-130 (for NANDP) labeling positions must allow the covalently attached nucleotides to swing out of the active site to allow MgATP to bind and be hydrolyzed. The finding that K^+-EDTA and NH_4^+-EDTA ATPase activities were negligible (Table 3) may reflect the known weaker binding of ATP to myosin in the absence of Mg^{2+} ions (Mandelkow & Mandelkow, 1973).

The actin-activated MgATPase of the photolabeled preparations was the same as the unmodified S1 (Table 3), consistent with the lack of effect of photolabeling of myosin upon the mechanical properties of fibers (Wang *et al.*, 1994). It was not expected that covalent modification at the edges of the active site pocket would have so little effect upon the ability of the S1 to hydrolyze ATP and to bind to actin. However, these data are consistent with the work of Peyser *et al.*, (1990), who showed that the incorporation of 0.8 mol of the 2-hydroxy-5-nitrobenzyl moiety into Trp-130 of rabbit skeletal S1 did not affect the actin-activated MgATPase. These combined experiments show that Trp-130 is not essential for ATP hydrolysis or for force generation in muscle. Thus, Trp-130 is a useful amino acid to attach probes to monitor this part of the myosin head.

We reasoned that the mobility and the accessibility to the solvent of the covalently attached probes should increase upon adopting the "out" position in the presence of ATP. Our polarization measurements (Figure 2) were consistent with MgATP, increasing the rotational mobility of CBHϵADP-S1. The acrylamide quenching data (Figure 3) shows that there is an increase in the estimated collisional quenching rate constant upon the addition of MgATP. These data strongly support the suggestion that the CBHϵADP remains outside the active site when the labeled S1 hydrolyzes MgATP. The positioning of the CBHϵADP into and out of the active site is reversible because the CBHϵADP-S1 is initially purified by the treatment with actin and MgATP, but when these constituents are removed from the solution, the purified CBHϵADP-S1 exhibits the fluorescence properties expected for the nucleotide bound at the active site. Thus, Ser-324 provides a second site to which probes can be attached without affecting myosin function.

The decrease in fluorescence intensity caused by the addition of MgATP to CBHϵADP-S1 (Figure 4) correlates well with the polarization (Figure 2) and quenching results

Scheme 1: Competition of ATP and the Tethered Analog for the Active Site

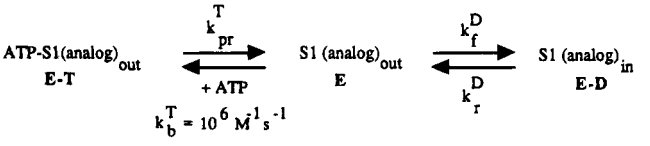

(Figure 3). At first glance, one may have predicted that the intensity should have increased when MgATP displaced the covalently bound probe into a more solvent exposed position. It is known that the fluorescence quantum yield of CBHϵADP reversibly bound or trapped on S1 with Vi is about 20% lower than the quantum yield of the free nucleotide (Cremo & Yount, 1987) and that the quantum yield of ϵADP is higher in aqueous solution (pH 7.0) than in various organic solvents (Secrist *et al.*, 1972). There are two factors that may account for the differences between these two studies and the experiments described here. First, the fluorophore is covalently attached to the protein, which may affect its fluorescence properties in an unexpected way. Second, it has been shown that CBH in the 2′ position of the ribose ring strongly quenches ϵADP fluorescence (Cremo & Yount, 1987). Therefore, the decrease in fluorescence upon repositioning the covalently attached probe out of the active site by MgATP is consistent with a rapid reequilibration (Griffin *et al.*, 1966; Neal *et al.*, 1990) from a state that favors the 3′-isomer to one that contains a mixture of both the 3′- and 2′-isomers.

The relatively large fluorescence intensity decrease upon the addition of MgATP was used to measure the affinity of the tethered CBHϵADP for binding to the active site. The MgATPase activity of the labeled S1, in which MgATP must displace the tethered diphosphate analog, can be described in terms of competition between ATP and the analog for the S1 active site (Scheme 1).

$S1(analog)_{out}$ stands for the configuration with the tethered diphosphate analog outside of the active site, *i.e.*, the labeled S1 has an empty binding site abbreviated as E. Similarly, $S1(analog)_{in}$ and $ATP\text{-}S1(analog)_{out}$ represent the active site of a labeled S1 occupied by the tethered analog or an ATP, abbreviated as E-D and E-T, respectively. k^D_f and k^D_r are the on rate and off rate of the binding processes involving only the tethered diphosphate analog. k^T_b is the on rate of ATP binding. Since the binding of ATP is not in equilibrium, but rather in a steady-state hydrolysis, k^T_{pr} represents the off rate of the hydrolysis products.

The ability of the bound analog to block the active site can be described in terms of an effective concentration of the tethered analog. The effective concentration is estimated by assuming that each attached ligand is free to move within a volume permitted by the length of the tether. If the CBHϵADP has full ability to move within a half-sphere of 15 Å (the dimension of the molecule from the tethering carbonyl to the end of β-phosphate or adenine ring) radius, then the geometry defines effective concentration of the diphosphate probe to be 240 mM. This effective concentration can be compared to that determined from competition with a free ligand, in this case MgADP, as discussed below. The occupancy of a labeled binding site by an ATP relative to that of the tethered analog, $P_{E\text{-}T}$ or $P_{E\text{-}D}$, is proportional to the on rate and the time that the nucleotide spends at the binding site, τ_T or τ_D, respectively, assuming that τ_T and τ_D

can be taken as the inverse of the corresponding off rates, *i.e.*, $1/k^{T}_{pr}$ and $1/k^{D}_{r}$. The ratio of $P_{E\text{-}T}$ to $P_{E\text{-}D}$ is expressed in

$$\frac{P_{E\text{-}T}}{P_{E\text{-}D}} = \frac{[ATP](k^{T}_{b})\tau_{T}}{[analog]_{eff}(k^{D}_{f})\tau_{D}} = \frac{[ATP]k^{T}_{b}/k^{T}_{pr}}{[analog]_{eff}k^{D}_{f}/k^{D}_{r}} \quad (4)$$

where $[analog]_{eff}$ stands for the effective concentration of the tethered diphosphate analog when it competes with ATP for an active site. If the experimentally measured maximum decrease in fluorescence intensity of CBHϵADP-S1 at 2 mM MgATP, ΔF_{max}, reflects near 100% occupancy by ATP, the intermediate intensity changes, *i.e.*, $\Delta F/\Delta F_{max}$, are then the measure of percentage of E-T in total labeled enzyme, $P_{E\text{-}T}/(P_{E\text{-}T} + P_{E\text{-}D})$. Consequently, eq 5 is a different form of

$$\frac{P_{E-T}}{(P_{E-T} + P_{E-D})[ATP]} = \frac{k^{T}_{b}/k^{T}_{pr}}{[analog]_{eff}k^{D}_{f}/k_{r}^{D}}\left(1 - \frac{P_{E-T}}{P_{E-T} + P_{E-D}}\right) \quad (5)$$

eq 4 that should correspond to the Scatchard equation (eq 6).

$$\frac{\Delta F}{\Delta F_{max}[ATP]} = K\left(1 - \frac{\Delta F}{\Delta F_{max}}\right) \qquad K = \frac{k^{T}_{b}/k^{T}_{pr}}{[analog]_{eff}k^{D}_{f}/k^{D}_{r}} \quad (6)$$

The Scatchard plot in the inset of Figure 5 gives a K value of 9.2×10^{3} M^{-1}. k^{D}_{f}/k^{D}_{r} can be estimated with the binding constant of Bz_{2}ϵADP (1.8×10^{5} M^{-1}) (Cremo & Yount, 1987). k^{T}_{b} is about 10^{6} M^{-1} s^{-1} (Geeves & Halsall, 1986). Since the product release is the rate-limiting step in an ATPase cycle, the off rate (k^{T}_{pr}) can be estimated by the MgATPase rate of 0.06 s^{-1} (Table 1). These numbers give an effective concentration of the tethered diphosphate analog as 10 mM, from eqs 5 and 6, assuming that the rate constants for association and dissociation are unchanged by the presence of the tether. The fact that the effective concentration measured by competition is much lower than that estimated from geometrical constraints indicates that the chemical bond between the analog and the protein significantly limits the ability of the analog to rebind to the active site. Either the rate of association is decreased or the rate of dissociation is increased (or both are affected) by the presence of the ligand.

Using a combination of ATPase assays, Vi complex stability, fluorescence polarization, and quenching, we were able to ask the question, "Does actin alone open the ATP binding pocket?". An opening of the pocket from the S1-ADP to the actoS1-ADP state is predicted by the model proposed by Rayment and co-workers (Rayment *et al.*, 1993a). Our covalently labeled preparations appear to be good models for the S1-ADP state, which is at the end of the power stroke. We saw no change in either the polarization (Figure 2) or the acrylamide quenching (Figure 3) upon the addition of actin to CBHϵADP-S1. Consistent with this finding, actin did not change the emission intensity of CBHϵADP-S1 (Figure 4). Therefore, our results suggest that the environment of the adenine ring in the S1-ADP and the actoS1-ADP states are not significantly different. We cannot rule out the possibility that the region of the active site pocket around the adenine ring opens or widens upon actin binding but that the environment around the adenine ring remains unchanged with respect to mobility and accessibility to solvent. We have constructed an energy-minimized model of ATP bound to the nucleotide-free structure of S1 (D. Lawson, I. Rayment, and R. Yount, unpublished observations). This model suggests that the adenine ring binds predominately to the 23-kDa NH_{2}-terminal fragment and little if any at all to the 50-kDa fragment on the other side of the active site entrance. On the basis upon this model and recognizing that the CBH group is attached to the 50-kDa fragment, a large opening or widening of the pocket would surely pull the adenine ring from its binding site on the 23-kDa fragment. This type of movement would have been detected by the fluorescence methods used here. Therefore, it appears that a large conformational change at the adenine binding portion of the active site is probably not involved in the power stroke. This conclusion was also reached from studies of fluorescent nucleotides bound reversibly to actomyosin (Franks-Skiba *et al.*, 1994; and same in preparation). However, actin binding did destabilize the Vi complexes of S1 photolabeled with both NANDP-S1 and CBHϵADP-S1 (Table 2). These results combined with the fluorescence studies above indicate that actin binding affects the γ-phosphate (Vi) binding site of myosin more strongly than the purine binding site. This effect likely reflects a critical step in the contraction cycle and gives additional insight into the molecular details of how actin binding effects product release from the myosin−ADP−Pi complex.

In conclusion, we have characterized two new covalently modified S1 preparations. The modifications were made specifically to residues at the edges of the active site pocket by using two photoreactive ADP analogs that react with amino acids at the ribose and adenine ring binding sites, respectively. These labeled S1 derivatives have two promising future applications. First, they promise to be good stable nucleotide bound forms of S1 for crystallization attempts. Second, with the proper probes attached, they can be used to examine the orientation of myosin crossbridges in muscle fibers during the power stroke. Finally, the active site region of other enzymes may be studied by the same approach after introduction of chromophoric or fluorescent photoaffinity substrate analogs as reporter groups.

ACKNOWLEDGMENT

We thank David Lawson for providing [^{3}H]NANTP and [^{32}P]NANDP. We wish to thank Jean Grammer, Dr. Bruce Kerwin, Mark Tibeau, and Tammy Stobb for helpful discussions and technical advice.

REFERENCES

Biosca, J. A., Greene, L. E., & Eisenberg, E. (1986) *J. Biol. Chem. 261*, 9793−9800.

Chalovich, J. M., & Eisenberg, E. (1982) *J. Biol. Chem. 257*, 2432−2437.

Cole, D. G., & Yount, R. G. (1990) *J. Biol. Chem. 265*, 22537−22546.

Cremo, C. R., & Yount, R. G. (1987) *Biochemistry 26*, 7524−7534.

Cremo, C. R., Grammer, J. C., & Yount, R. G. (1989) *J. Biol. Chem. 264*, 6608−6611.

Franks-Skiba, K., Hwang, T., & Cooke, R. (1994) *Biophys. J. 66*, A347.
Geeves, M. A. (1989) *Biochemistry 28*, 5864−5871.
Geeves, M. A., & Halsall, D. J. (1986) *Proc. R. Soc. London B229*, 85−95.
Geeves, M. A., Goody, R. S., & Gutfreund, H. (1984) *J. Muscle Res. Cell Motil. 5*, 351−361.
Goodno, C. (1979) *Proc. Natl. Acad. Sci. U.S.A. 76*, 2620−2624.
Goodno, C. C., & Taylor, E. W. (1982) *Proc. Natl. Acad. Sci. U.S.A. 79*, 21−25.
Grammer, J., & Yount, R. G. (1991) *Biophys. J. 59*, 226a.
Grammer, J. C., Cremo, C. R., & Yount, R. G. (1988) *Biochemistry 27*, 8408−8415.
Grammer, J. C., Kuwayama, H., & Yount, R. G. (1993) *Biochemistry 32*, 5725−5732.
Greene, L. E., & Eisenberg, E. (1980) *J. Biol. Chem. 255*, 543−548.
Griffin, B. E., Jarman, M., Reese, C. B., Sulston, J. E., & Trentham, D. R. (1966) *Biochemistry 5*, 3638−3649.
Lanzetta, P. A., Alvarez, L. J., Reinach, P. S., & Candia, O. A. (1979) *Anal. Biochem. 100*, 95−97.
Lehrer, S. S., & Leavis, P. C. (1978) *Methods Enzymol. 49*, 222.
Mahmood, R., Elzinga, M., & Yount, R. G. (1989) *Biochemistry 28*, 3989−3995.
Mandelkow, E.-M., & Mandelkow, E. (1973) *FEBS Lett. 33*, 161−166.
Millar, N. C., & Geeves, M. A. (1988) *Biochem. J. 249*, 735−743.
Nakamaye, K. L., Wells, J. A., Bridenbaugh, R. L., Okamoto, Y., & Yount, R. G. (1985) *Biochemistry 24*, 5226−5235.
Neal, S. E., Eccleston, J. F., & Webb, M. R. (1990) *Proc. Natl. Acad. Sci. U.S.A. 87*, 3562.
Okamoto, Y., & Yount, R. G. (1985) *Proc. Nat. Acad. Sci. U.S.A. 82*, 1575−1579.
Pardee, J. D., & Spudich, J. A. (1982) *Methods Enzymol. 85*, 164−182.
Penefsky, H. S. (1977) *J. Biol. Chem. 252*, 2891−2899.
Peyser, Y. M., Muhlrad, A., & Werber, M. M. (1990) *FEBS Lett. 259*, 346−348.
Rayment, I., Holden, H. M., Whittaker, M., Yohn, C. B., Lorenz, M., Holmes, K. C., & Milligan, R. A. (1993a) *Science 261*, 58−65.
Rayment, I., Rypniewski, W. R., Schmidt-Base, K., Smith, R., Tomchick, D. R., Benning, M. M., Winkelmann, D. A., Wesenberg, G., & Holden, H. M. (1993b) *Science 261*, 50−58.
Secrist, J. A. I., Barrio, J. R., Leonard, N. J., & Weber, G. (1972) *Biochemistry 11*, 3499−3506.
Siemankowski, R. E., & White, H. D. (1984) *J. Biol. Chem. 259*, 5045−5053.
Stern, O., & Volmer, M. (1919) *Phys. Z. 20*, 183.
Trybus, K. M., & Taylor, E. W. (1980) *Proc. Natl. Acad. Sci. U.S.A. 77*, 7209−7213.
Wagner, P. D., & Yount, R. G. (1975) *Biochemistry 14*, 1900−1907.
Wagner, P. D., & Weeds, A. (1977) *J. Mol. Biol. 109*, 455−473.
Wang, D., Luo, Y., Pate, E., Cooke, R., & Yount, R. G. (1994) *Biophys. J. 66*, A77.
Weeds, A. G., & Taylor, R. S. (1975) *Nature 257*, 54−56.
Wells, J. A., Werber, M. M., & Yount, R. G. (1979) *Biochemistry 18*, 4800−4805.
Yount, R. G., Cremo, C. R., Grammer, J. C., & Kerwin, B. A. (1992) *Philos. Trans. R. Soc. London B336*, 55−61.

BI941426R